First Reported Correlation between the Calculated Gas-Phase Proton Macroaffinities of Some Metal Complexes with Their Measured Formation Constants in Solution: Zn(II) Complexes of a Series of Tripodal Aliphatic Tetraamines

Sadegh Salehzadeh,*,† Mehdi Bayat,† and Michael D. Ward‡

Faculty of Chemistry, Bu-Ali Sina University, Hamedan, Iran, and Department of Chemistry, University of Sheffield, Sheffield, S3 7HF, United Kingdom

Received: October 1, 2007; In Final Form: January 17, 2008

A theoretical study on the first protonation step of a series of metal complexes with the general formula $\{M(N[(CH_2)_nNH_2][(CH_2)_mNH_2][(CH_2)_pNH_2])^{2+}\}$ ($n = m = p = 2$, tren; $n = 3$, $m = p = 2$, pee; $n = m = 3$, $p = 2$, ppe; $n = m = p = 3$, tpt; $n = 2$, $m = 3$, $p = 4$, epb; and $n = m = 3$, $p = 4$, ppb; and $M = Zn^{2+}$) was reported using both the Hartree−Fock and DFT (B3LYP) levels of theory. For the first time, two kinds of our recently published definitions for gas-phase proton affinities of polybasic ligands, proton microaffinity and proton macroaffinity, were extended to their metal complexes. There is a good correlation between the calculated gas-phase proton macroaffinities and the corresponding formation constants in solution.

Introduction

Recently, we applied three newly defined gas-phase proton affinities for polybasic molecules: proton microaffinity, proton macroaffinity, and proton overall affinity. We established an equation, eq 1, for the calculation of proton macroaffinities, $\overline{PA}_n$, of polyamine molecules with any type of symmetry[1]

$$\overline{PA_n} = \frac{\sum_{j=1}^{l}\sum_{i=1}^{m} PA_{n,i}R_{n,j}S_{n,i}}{\sum_{j=1}^{l}\sum_{i=1}^{m} R_{n,j}S_{n,i}} \quad (1)$$

where $R_{n,j} = \sum_{j=1}^{K} R_{n-1,j}S_{n-1,j}$.

This formula shows that $\overline{PA}_n$ not only depends on the proton microaffinities, $PA_{n,i}$, and the relative abundance of the species that is related to them, $R_{n,j}$, but also to the available identical sites that undergo protonation, $S_{n,i}$. Obviously, the relative abundance of the initial neutral molecule, $R_{1,1}$, is 1, and that of any other species depends on both the relative abundance of the previous species, $R_{n-1,j}$, and the available identical sites on them, $S_{n-1,j}$, which are involved in its formation.

The proton overall affinity, PA_{ov}, also is defined as the negative of the electronic energy difference between L and its fully protonated form (herein, H_4L^{4+}) together with a correction for the difference in zero-point energies. According to Hess's law, the summation of the calculated proton macroaffinities for one polybasic molecule ($\overline{PA}_{ov}$, see eq 2) must be the same as or very close to its proton overall affinity, PA_{ov}

$$\overline{PA}_{ov} = \sum_{n=1}^{m} \overline{PA_n} \quad (2)$$

For first time, we showed that there is a good correlation between the calculated gas-phase proton macroaffinities and the corresponding solution/protonation macroconstants (see eqs 3 and 4) for a number of tripodal tetraamines (see Figure 1; tren, pee, ppe, tpt, and ppb) that in recent years have been of interest.[2−6] Furthermore, the correlation between the calculated log $\overline{PA}_{ov}$ and the measured log β_4 (see eq 5) particularly was excellent for the latter tetraamines

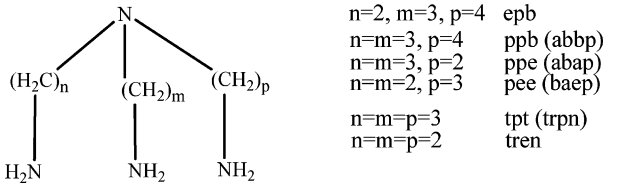

Figure 1. Structures of the tripodal tetraamine ligands investigated here along with their common abbreviations.

$$H_{n-1}L^{(n-1)+} + H^+ \rightleftharpoons H_nL^{n+} \quad (3)$$

$$K_n = \frac{[H_nL^{n+}]}{[H_{n-1}L^{(n-1)+}][H^+]} \quad (4)$$

$$\beta_n = K_1K_2...K_n \quad (5)$$

Very recently, we showed that our definitions for proton affinities of polybasic molecules are reliable for more bulky polybasic molecules. We also investigated the Maxwell−Boltzmann equation (eq 6) for the calculation of the probability distribution (x_i) of different n protonated species in the protonation steps of the latter molecules. We showed that the equation (eq 1) for the calculation of proton macroaffinities for this type of polybasic molecule is more reliable than other equations including the Boltzmann distribution (eqs 7 and 8)[7]

$$x_i = \frac{e^{-\Delta^{G_i^0}/RT}}{\sum_{i=1}^{n} e^{-\Delta^{G_i^0}/RT}} \quad (6)$$

* Corresponding author. Fax: +98(811)8257407; e-mail: saleh@basu.ac.ir.
† Bu-Ali Sina University.
‡ University of Sheffield.

10.1021/jp709603r CCC: $40.75
Published on Web 03/19/2008

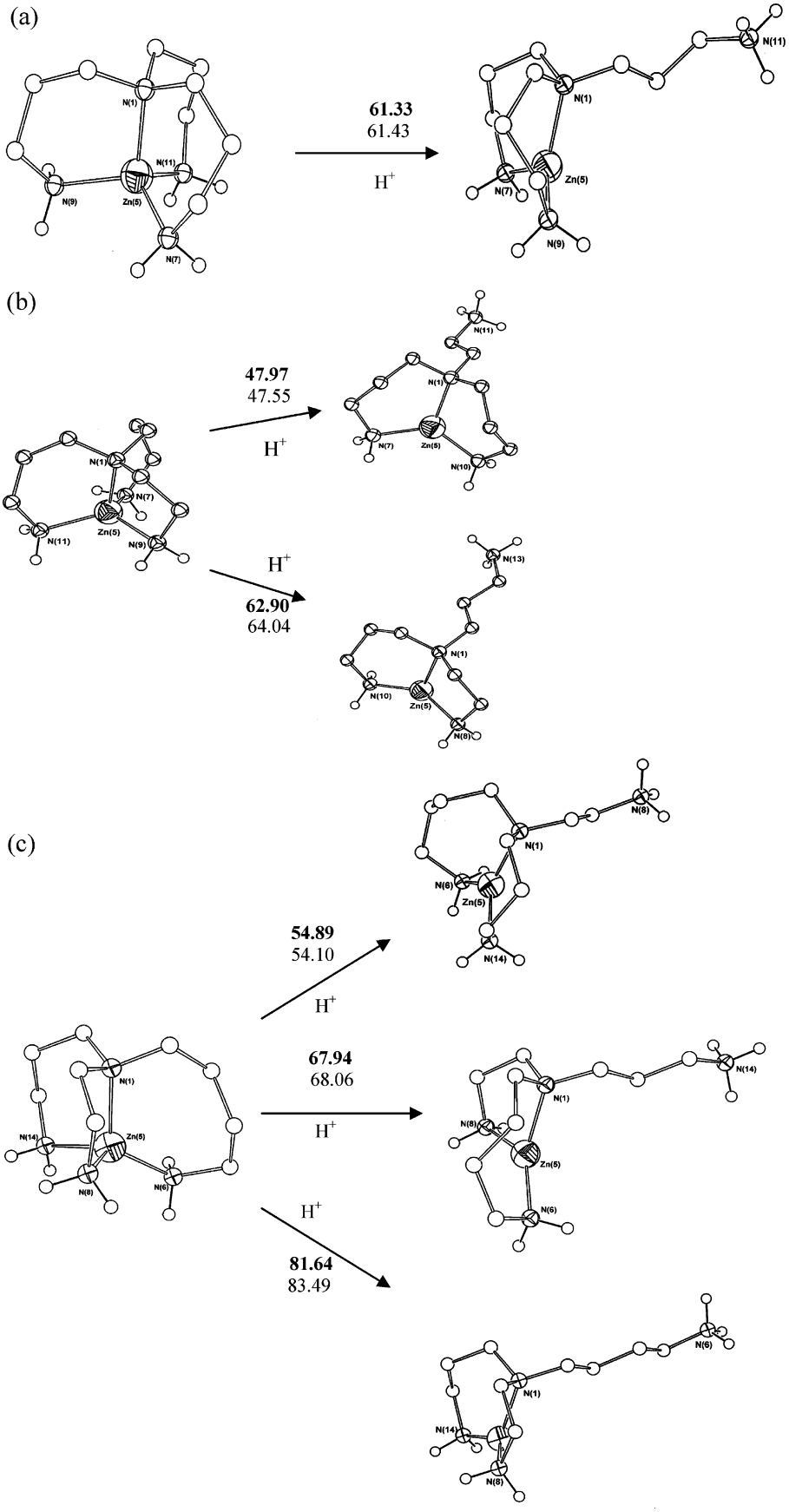

Figure 2. Illustration of all possible paths for the gas-phase first protonation step of $Zn(tpt)^{2+}$ (a), $Zn(ppe)^{2+}$ (b), and $Zn(epb)^{2+}$ (c) along with calculated proton microaffinities (kcal mol^{-1}). Calculations were performed at the B3LYP (bold) and HF (plain text) levels using the 6-31G* basis set for C, H, and N atoms and Lanl2dz for metal ions.

TABLE 1: Calculated Zero-Point Energies, Total Energies, Electronic Energy (Hartree), and Proton Microaffinity PA_i of the ZnL^{2+} Complexes with the 6-31G* Basis Set for C, H, and N and the LanL2DZ Basis Set for the Metal Ion

		B3LYP			
species[a]	protonated site	ZPE	E_0	E_{el}	PA_i
$Zn(L222)^{2+}$		0.270286	−2237.066459	−2237.3367454	
$Zn(L222H)^{3+}$	**2**	0.282257	−2237.131397	−2237.4136541	40.75
$Zn(L322)^{2+}$		0.299278	−2276.362303	−2276.6615812	
$Zn(L322H)^{3+}$	**2**	0.310961	−2276.434913	−2276.7458740	45.56
$Zn(L322H)^{3+}$	**3**	0.311150	−2276.447607	−2276.7587566	53.52
$Zn(L332)^{2+}$		0.328020	−2315.654502	−2315.9825214	
$Zn(L332H)^{3+}$	**2**	0.339661	−2315.730955	−2316.0706160	47.97
$Zn(L332H)^{3+}$	**3**	0.340098	−2315.754747	−2316.0948450	62.90
$Zn(L333)^{2+}$		0.356946	−2354.945215	−2354.9452150	
$Zn(L333H)^{3+}$	**3**	0.368470	−2355.042957	−2355.4114268	61.33
$Zn(L433)^{2+}$		0.385923	−2394.224877	−2394.6108001	
$Zn(L433H)^{3+}$	**3**	0.397684	−2394.334219	−2394.7319037	68.61
$Zn(L433H)^{3+}$	**4**	0.397782	−2394.362301	−2394.7600824	86.23
$Zn(L432)^{2+}$		0.356776	−2354.940646	−2355.2974225	
$Zn(L432H)^{3+}$	**2**	0.368562	−2355.028123	−2355.3966850	54.89
$Zn(L432H)^{3+}$	**3**	0.368465	−2355.048915	−2355.4173802	67.94
$Zn(L432H)^{3+}$	**4**	0.368655	−2355.070747	−2355.4394014	81.64

[a] L222, L322, L332, L333, L433, and L432 correspond to tren, pee, ppe, tpt, ppb, and epb tripodal tetraamines, respectively.

$$\overline{PA_n} = \frac{\sum_{i=1}^{n} PA_{n,i}x_i}{\sum_{i=1}^{n} x_i} \tag{7}$$

$$\overline{PA_n} = \frac{\sum_{j=1}^{l}\sum_{i=1}^{m} PA_{n,i}R_{n,j}S_{n,i}x_i}{\sum_{j=1}^{l}\sum_{i=1}^{m} R_{n,j}S_{n,i}x_i} \tag{8}$$

We were interested in investigating as to whether our definitions for proton affinities of polybasic molecules are reliable not only for a free polydentate ligand but also for the ligand coordinated to the metal ion. It is clear that the protonation of the coordinated donor atom will remove it from the metal ion. Obviously, as the stability of a particular metal−ligand complex increases (a result of ligand−metal bonding interactions), the proton affinity of the coordinated ligand will be decreased. Thus, we were interested in knowing as to whether the formation constants (see eq 9) of metal complexes of a series of related ligands can be correlated with the proton macroaffinities of the coordinated ligands. Thus, in this paper, we report a theoretical study of the first protonation step of a series of metal complexes of the general formula $\{Zn(N[(CH_2)_nNH_2][(CH_2)_mNH_2][(CH_2)_pNH_2])\}^{2+}$ ($n = m = p = 2$, tren; $n = 3$, $m = p = 2$, pee; $n = m = 3$, $p = 2$, ppe; $n = m = p = 3$, tpt; $n = 2$, $m = 3$, $p = 4$, epb; and $n = m = 3$, $p = 4$, ppb; Figure 1) using Hartree−Fock and DFT (B3LYP). These systems were selected not only because of our own interest in the synthesis and application of such ligands[2−6] but also because the experimentally measured formation constants for a series of metal complexes of these interesting ligands in solution are available[4]

$$M^{n+} + L \rightleftharpoons ML^{n+}$$

$$K_f = \frac{[ML^{n+}]}{[M][L]} \tag{9}$$

Computational Methods

The geometries of all complexes were fully optimized at both Hartree−Fock and DFT (B3LYP)[8] levels of theory using the Gaussian 98 set of programs.[9] The standard 6-31G* basis set was used for C, H, and N. The Lanl2dz basis set was used for metal ions. This basis set includes the effective core potential (ECP) for metal ions. Vibrational frequency analyses, calculated at the same level of theory, indicated that optimized structures are located at the stationary points corresponding to local minima without any imaginary frequency. Calculations were performed on a Pentium-PC computer with a 3600 MHz processor. A starting molecular mechanics structure for the ab initio calculations was obtained using the HyperChem 5.02 program.[10]

Results and Discussion

The proton affinity of a monobasic neutral ligand at 0 K is defined as the negative of the electronic energy difference between HL^+ and L together with a correction for difference in zero-point energies. To convert the 0 K value to 298 K, one has to include thermal corrections for the translational, rotational, and vibrational energies and a correction for the change in the number of molecules assuming ideal gas behavior.[11] Defined in these ways, the proton affinity of L is a positive number; the more positive the number, the greater the energy gained by the system upon association of H^+ with L is.

For each polybasic molecule, there are several different sites at which protonation can occur; protonation of different sites will release different amounts of energy. Recently, we used the term microaffinity for the protonation of one special site in a polybasic molecule, and in the present work, we used the same term for the corresponding metal complexes. For the complexes in this paper, protonation could occur at either the bridgehead (tertiary) amine N atom or at one of the primary amine N atoms; furthermore, if the three arms of the ligand are not the same, there will be a choice as to which primary amine is protonated first. Protonation of the tertiary amine N atoms is energetically disfavored as compared to protonation of one of the primary amine sites. This is because of the electrostatic interaction between the protonated amine cation and the metal center. As can be seen in Figure 2, the primary amine group, upon protonation, is free to move away significantly from the metal cation, but the tertiary nitrogen atom, which is constrained by

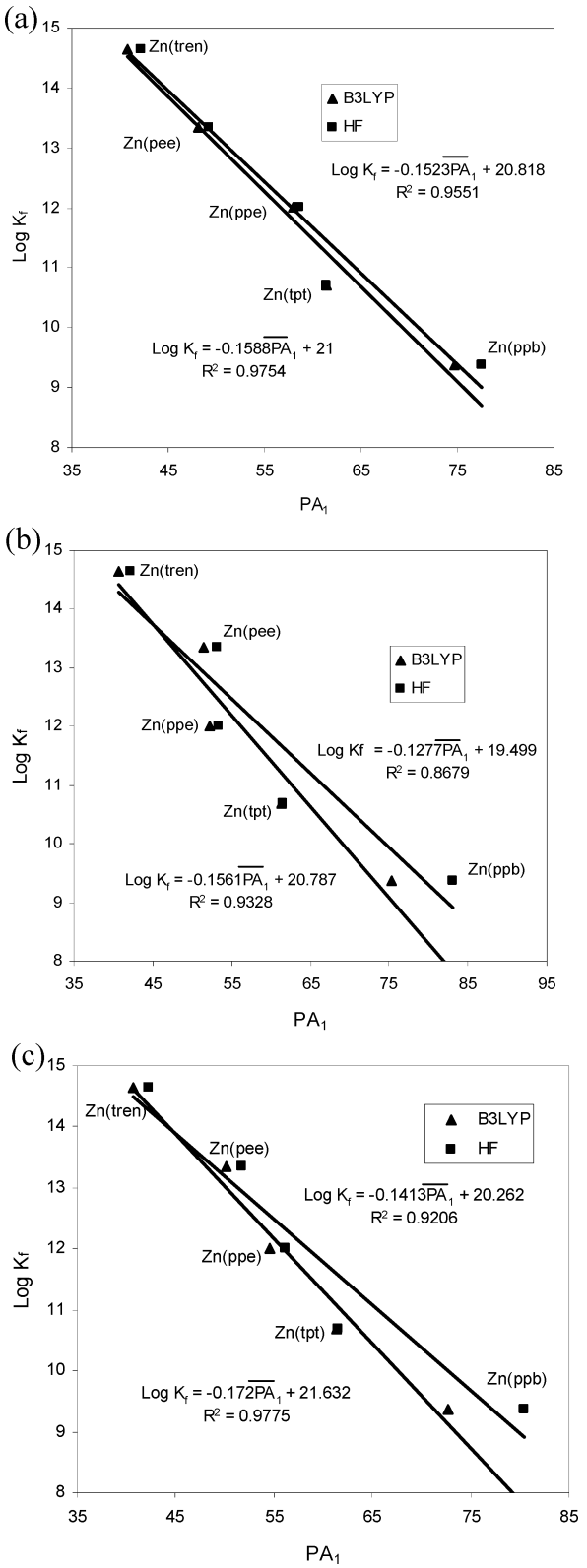

Figure 3. Correlation of log K_f vs calculated $\overline{PA_1}$ for the first protonation step of Zn complexes with tren, pee, ppe, tpt, and ppb at both HF and B3LYP/6-31G* levels of theory using LanL2DZ for metal ions. Panels a−c were calculated using eqs 10−12, respectively.

being connected to three coordinated primary amine groups, is not free to move away from the metal ion upon protonation but is held close to it. Thus, the involvement of the tertiary amine N atom in first protonation step of these complexes can be ignored, and herein, we consider only the protonation of the primary amine groups in these complexes. The number of proton microaffinities in the first protonation step of the complexes of polybasic ligands depends not only upon the number of basic sites but also upon the symmetry of the complexes.[12] The complexes investigated here belong to $M(AB_3)$ [i.e., M(tren) and M(tpt)], $M(AB_2C)$ [i.e., M(pee), M(ppe), and M(ppb)], and M(ABCD) [i.e., M(epb)] general types, in which the bridgehead tertiary amine atom is denoted as A, and the primary amine sites are donted as B/C/D. According to the previous discussion, if we assume that the tertiary nitrogen atom (A) does not undergo protonation, then we have one, two, and three different microaffinities, respectively, for the latter general types. One, two, and three different paths for protonation of latter general types are shown in Figure 2 for M(tpt), M(ppe), and M(epb), respectively.

In the present case, where we study only the first protonation step of the metal complexes, we can use the following simple form of eqs 1, 7, and 8:

$$\overline{PA_1} = \frac{\sum_{i=1}^{m} PA_i S_i}{\sum_{i=1}^{m} S_i} \tag{10}$$

$$\overline{PA_1} = \frac{\sum_{i=1}^{m} PA_i X_i}{\sum_{i=1<\mathrm{bu}>m} X_i} \tag{11}$$

$$\overline{PA_1} = \frac{\sum_{i=1}^{m} PA_i S_i X_i}{\sum_{i=1}^{m} S_i X_i} \tag{12}$$

In eq 10, PA_i is one of the calculated proton microaffinities in step 1, and S_i denotes the available identical sites to undergo protonation. In eqs 11 and 12, in contrast to eq 10, the population of the various species (x_i) is considered; this is evaluated from the computed Gibbs energies through a Boltzmann distribution. Whereas in the case of eq 11, the proton macroaffinities are calculated mainly according to a Boltzmann distribution, in eq 12, the latter distribution is added to eq 10. For the calculation of proton macroaffinities in each protonation step of the amine, in the case of eq 11, all proton microaffinities in that step and the population of the related species are considered. On the other hand, in the case of eq 12, in addition to all proton microaffinities and the population of the related species, S_i also is considered.

The following results were obtained from the study of proton microaffinities and the calculation of the first proton macroaffinity of the metal complexes using eqs 10−12: (1) For all complexes, the smallest calculated proton microaffinity is related to the amine group on the coordinated ethylene arm, and the greatest one is related to the amine group on the butylene arm (see Table 1). This is consistent with the fact that seven-membered chelate rings are less stable than six-membered rings and that both are less stable than five-membered chelate rings.[4,13] (2) As can be seen in Table 2, the smallest proton macroaffinity is calculated for the $[Zn(tren)]^{2+}$ complex. In fact, the order of the first proton macroaffinity for the Zn^{2+} complexes is [Zn-

TABLE 2: Comparison of Predicted Formation Constant for $Zn(epb)^{2+}$ with Measured Formation Constants for Other Zn Complexes of Tripodal Ligands Studied Here,[a] along with Calculated Gas-Phase Proton Macroaffinities (kcal mol^{-1}) for the First Step of Protonation of Ligands and Corresponding Complexes[b]

		$\overline{PA}_1$ $(ZnL)^{2+}$						
L	log K_f $(ZnL)^{2+}$	eq 10		eq 11		eq 12		$\overline{PA}_1$ (L)[c]
tren	14.65	**40.75**	42.19	**40.75**	42.19	**40.75**	42.19	**222.00**
pee	13.35	**48.20**	49.23	**51.43**	53.21	**50.21**	51.75	**225.30**
ppe	12.01	**57.92**	58.55	**52.19**	53.29	**54.55**	56.07	**231.00**
tpt	10.7	**61.33**	61.43	**61.33**	61.43	**61.33**	61.43	**235.80**
ppb	9.37	**74.75**	77.48	**75.29**	82.99	**72.74**	80.38	**243.60**
epb	**10.54** (10.38)[d]	**68.16**	68.55	**65.98**	71.42	**65.98**	71.42	**242.00**

[a] Experimental data were derived from ref 4. [b] Calculations were performed at the B3LYP (bold) and HF (plain text) levels using the 6-31G* basis set for C, H, and N atoms and LanL2DZ for the metal ion. [c] Data were derived from ref 1. [d] Predicted formation constants for the $Zn(epb)^{2+}$ complex at B3LYP (bold) and HF (plain text) levels of theory using eq 1.

$(tren)]^{2+}$ < $[Zn(pee)]^{2+}$ < $[Zn(ppe)]^{2+}$ < $[Zn(tpt)]^{2+}$ < $[Zn(ppb)]^{2+}$. The reason for this order must be that the tren complexes have three five-membered chelate rings, the pee complexes have two five- and one six-membered chelate rings, ppe complexes have one five- and two six-membered chelate rings, tpt complexes have three six-membered chelate rings, and ppb complexes have two six- and one seven-membered chelate rings. It is interesting that the order of stability of the latter complexes is $[Zn(tren)]^{2+}$ > $[Zn(pee)]^{2+}$ > $[Zn(ppe)]^{2+}$ > $[Zn(tpt)]^{2+}$ > $]Zn(ppb)]^{2+}$ (i.e., completely opposite to the observed trend for their proton macroaffinity). The latter observation confirms our assumption that there is a correlation between the proton affinity of a complex and its stability constant. As can be seen in Figure 3, there is a good correlation between the measured log K_f value versus the one calculated for the first protonation steps of the Zn^{2+} complexes investigated here. As can be seen in Figure 3, the calculated proton macroaffinities using eq 10 have good correlations with the experimental formation constants in both HF and DFT computations.

The latter observation has allowed us to predict the formation constant for the Zn^{2+} complex of the totally asymmetric ligand epb by using eq 10. It would be interesting if we compared the $[Zn(tpt)]^{2+}$ and $[Zn(epb)]^{2+}$ complexes. Both ligands in these two complexes have nine methylene groups, but there are three equivalent six-membered chelate rings in first complex and three different chelate rings in the second one. Whereas the five-membered ring in $[Zn(epb)]^{2+}$ is more stable than the six-membered ring in $[Zn(tpt)]^{2+}$, its seven-membered chelate ring is considerably less stable. As expected, the predicted formation constant values for $[Zn(epb)]^{2+}$ are slightly smaller than those for $[Zn(tpt)]^{2+}$.

Conclusion

The results of this work show that the reliable theoretical calculation of the gas-phase first proton macroaffinity of polybasic molecules coordinated to a metal ion, according to proton microaffinity analysis, is possible. The formation constants of metal complexes of a series of related ligands can be correlated with the proton macroaffinities of the coordinated ligands.

Supporting Information Available: Calculated zero-point energies, Gibbs free energies, and Cartesian coordinates. This material is available free of charge via the Internet at http://pubs.acs.org.

Note Added after ASAP Publication. This article was released ASAP on March 19, 2008. Equation 2 has been modified. The sentence above equation 1 and the sentence below equation 12 have also been modified. The corrected version posted on April 24, 2008.

References and Notes

(1) Salehzadeh, S.; Bayat, M. *Chem. Phys. Lett*. **2006**, *427*, 455.

(2) Salehzadeh, S.; Javarsineh, S. A.; Keypour, H. *J. Mol. Struct*. **2006**, *785*, 54.

(3) Salehzadeh, S.; Nouri, S. M.; Keypour, H.; Bagherzadeh, M. *Polyhedron* **2005**, *24*, 1478.

(4) Keypour, H.; Dehdari, M.; Salehzadeh, S. *Transition Met. Chem*. **2003**, *28*, 425.

(5) Keypour, H.; Salehzadeh, S.; Pritchard R. G.; Parish, R. V. *Inorg. Chem*. **2000**, *39*, 5787.

(6) Keypour, H.; Salehzadeh, S. *Transition Met. Chem*. **2000**, *25*, 204.

(7) Salehzadeh, S.; Bayat, M.; Hashemi, M. *J. Phys. Chem. A* **2007**, *111*, 8188.

(8) Becke, A. D. *J. Chem. Phys*. **1993**, *98*, 5648.

(9) Frisch, M. J.; Trucks, G. W.; Schlegel, H. B.; Scuseria, G. E.; Robb, M. A.; Cheeseman, J. R.; Montgomery, J. A., Jr.; Vreven, T.; Kudin, K. N.; Burant, J. C.; Millam, J. M.; Iyengar, S. S.; Tomasi, J.; Barone, V.; Mennucci, B.; Cossi, M.; Scalmani, G.; Rega, N.; Petersson, G. A.; Nakatsuji, H.; Hada, M.; Ehara, M.; Toyota, K.; Fukuda, R.; Hasegawa, J.; Ishida, M.; Nakajima, T.; Honda, Y.; Kitao, O.; Nakai, H.; Klene, M.; Li, X.; Knox, J. E.; Hratchian, H. P.; Cross, J. B.; Adamo, C.; Jaramillo, J.; Gomperts, R.; Stratmann, R. E.; Yazyev, O.; Austin, A. J.; Cammi, R.; Pomelli, C.; Ochterski, J. W.; Ayala, P. Y.; Morokuma, K.; Voth, G. A.; Salvador, P.; Dannenberg, J. J.; Zakrzewski, V. G.; Dapprich, S.; Daniels, A. D.; Strain, M. C.; Farkas, O.; Malick, D. K.; Rabuck, A. D.; Raghavachari, K.; Foresman, J. B.; Ortiz, J. V.; Cui, Q.; Baboul, A. G.; Clifford, S.; Cioslowski, J.; Stefanov, B. B.; Liu, G.; Liashenko, A.; Piskorz, P.; Komaromi, I.; Martin, R. L.; Fox, D. J.; Keith, T.; Al-Laham, M. A.; Peng, C. Y.; Nanayakkara, A.; Challacombe, M.; Gill, P. M. W.; Johnson, B.; Chen, W.; Wong, M. W.; Gonzalez, C.; Pople, J. A. *Gaussian 98*, revision B.04; Gaussian, Inc.: Pittsburgh, PA, 1998.

(10) *HyperChem*, version 5.02; Hypercube, Inc.: Gainesville, FL, 1997.

(11) Rusted, J. R.; Dixon, D. A.; Kubicki, J. D.; Felmy, A. R. *J. Phys. Chem. A* **2000**, *104*, 4051.

(12) Szakać, Z.; Noszaí, B. *J. Math. Chem*. **1999**, *26*, 139.

(13) Barbucci, R.; Paoletti, P.; Vacca, A. *Inorg. Chem*. **1975**, *14*, 302.